Atmospheric
Measurement
Techniques
Discussions

Open Access

Supplement of

The "dual-spot" Aethalometer: an improved measurement of aerosol black carbon with real-time loading compensation

L. Drinovec et al.

Correspondence to: L. Drinovec (luka.drinovec@aerosol.si) and G. Močnik (grisa.mocnik@aerosol.si)

24   **Filter loading effect for different measurement sites and seasons**

25   The filter loading effect is determined by the *BC*(*ATN*) method for measurement campaigns

26   conducted at different type of measurement site (roadside, urban background, rural background,

27   regional background) in Klagenfurt (Austria), Anaheim (USA), Payerne (Switzerland), Sonnblick

28   (Austria), Kathmandu (Nepal). Uncompensated *BC* data as measured by the AE33 with the detector

29   under spot S1 was fitted using a linear function in the *ATN* range from 4.4 to 45. The filter loading

30   effect is determined as the relative slope *RS* (Eq. 2).

31

32

33
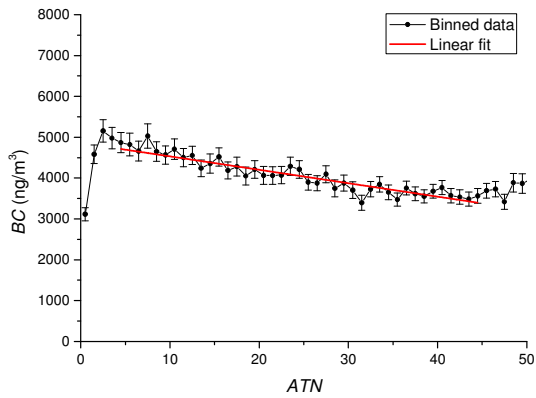
Figure S1. *BC*(*ATN*) analysis of the filter loading effect for the campaign in Klagenfurt (Austria) from 1-12 March 2012. The Klagenfurt station is located at Völkermarkter Strasse (46°37'32.1"N 14°19'05.7"E, 446 m ASL). The station is located in the middle of a crossroad and is strongly influenced by local traffic. During winter the site is strongly influenced by biomass burning from residential heating. Average BC data for each ATN bin (1 ATN unit wide) and the linear fit of the raw data are presented.

41
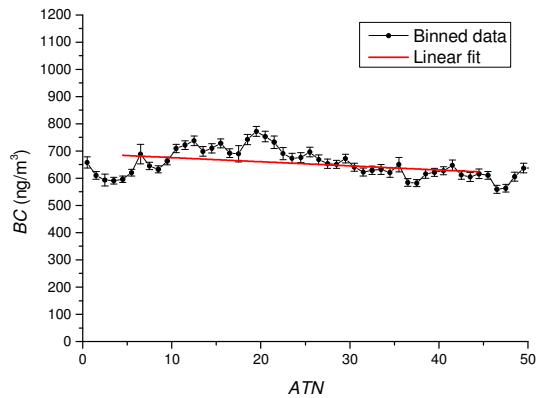
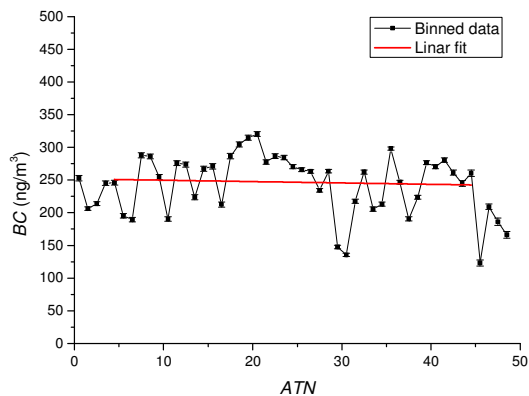Figure S2. *BC*(*ATN*) analysis of the filter loading effect for a campaign in Anaheim (California, USA) from 1-9 July 2012. The Anaheim station is located in an urban environment (33° 49' 50" N, 117° 56' 18"W, 39 m ASL). Average BC data for each ATN bin (1 ATN unit wide) and the linear fit of the raw data are presented.

46
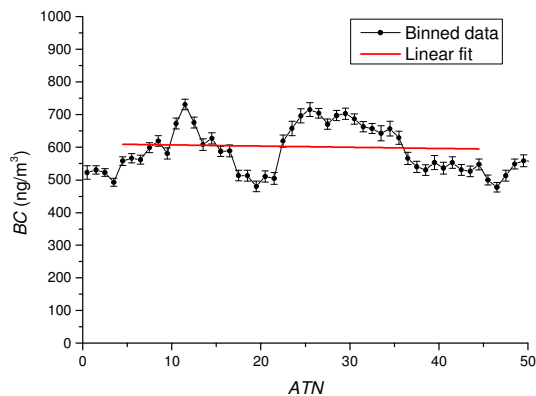
Figure S3. *BC*(*ATN*) analysis of the filter loading effect for campaign in Payerne (Switzerland) from 15 June – 5 July 2012. The Payerne aerological station (46.82 ° N, 6.95 ° E, 491 m ASL) is a rural background air quality monitoring station located in Southwestern Switzerland, on the Swiss plateau between the Jura and the Alps. It lies about 1 km south-east of the small rural town of Payerne. The site is surrounded by agricultural fields (grassland and crops), forests and small villages. Average BC data for each ATN bin (1 ATN unit wide) and the linear fit of the raw data are presented.

54

Figure S4. *BC*(*ATN*) **analysis of the filter loading effect for campaign in Sonnblick (Austria) from 1**

July to 31 August 2013. The Sonnblick observatory is a background station located in the high

alpine environment (47°03'15''N, 12°57'27''E, 3106 m ASL). Measurements at this location allow

the determination of the composition of the mid-troposphere, frequently reaching into the free

troposphere. Average BC data for each ATN bin (1 ATN unit wide) and the linear fit of the raw data

are presented.

61

62
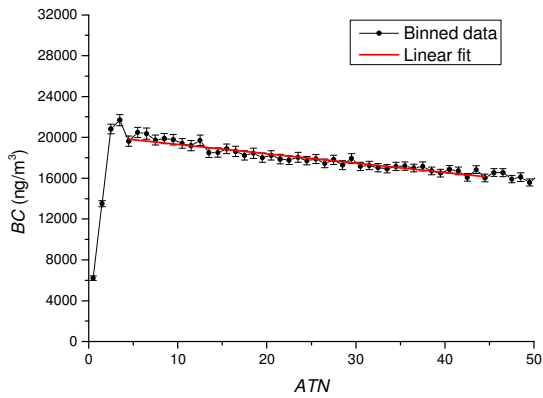
Figure S5. *BC*(*ATN*) analysis of the filter loading effect for campaign in Kathmandu (Nepal) from 1-

31 February 2013. Located at Bode (27.68°N, 85.39°E, 1345 m ASL) in the agricultural-residential

setting), this site often receives the outflows of three major cities in the valley (Kathmandu,

Lalitpur and Bhaktapur) and occasionally receives regional air masses. BC emissions originate from

a combination of residential cooking, heating, brick factories, small diesel-powered generator sets,

open burning of solid waste and traffic. Average BC data for each ATN bin (1 ATN unit wide) and

the linear fit of the raw data are presented.

73 **Table S1. Average filter loading effect as determined with the *BC*(A*TN*) analysis for different**

74 **measurement sites and seasons.**

Location	*BC*(A*TN*) relative slope *RS*	Site description	Season
Klagenfurt (Austria)	- 0.0069 +/- 0.0007	Roadside	Winter
Anaheim (USA)	- 0.0033 +/- 0.0003	Urban	Summer
Payerne (Switzerland)	- 0.0013 +/- 0.0004	Rural background	Summer
Sonnblick (Austria)	- 0.0017 +/- 0.0002	Regional background	Summer
Kathmandu (Nepal)	- 0.0047 +/- 0.0003	Urban	Winter

75

76

77

78

79
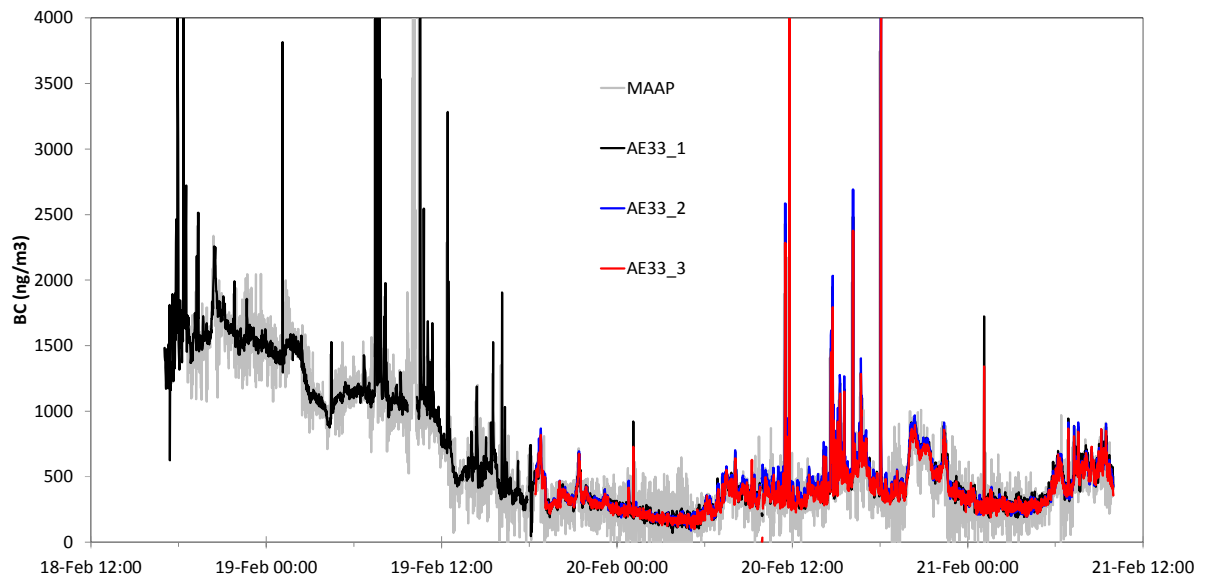
Figure S6. Time-series of the ACTRIS inter-comparison, showing AE33 and MAAP measurements of

81 **BC.**

82

83 **Table S2. Mass absorption cross-section values used in the AE33.**

Channel	Wavelength (nm)	σ_{air}(m^2/g)
1	370	18.47
2	470	14.54
3	520	13.14
4	590	11.58
5	660	10.35
6	880	7.77
7	950	7.19

84

85 The mass absorption cross-section values σ_{air} used in the Aethalometer assume an inverse

86 dependence on the wavelength – that is, a "black" sample with an Ångström exponent equal to unity

87 (Moosmüller et al., 2011). The relationship between the absorption and mass was determined by

88 optical measurements of transmission and thermal measurements of samples, where the non-

89 refractory constituents of the carbonaceous sample were removed (Gundel et al., 1984) –

90 measurements in the infra-red part of the spectrum should therefore be used to convert the optical

91 measurement into the mass concentration, as the contribution of sample components other than

92 black carbon is negligible at these wavelengths (Sandradewi et al., 2008a; Sandradewi et al., 2008b;

93 Fialho et al., 2005; Yang et al., 2009; and references therein). The relationship between the mass

94 concentration of BC and the optical absorption can be determined by comparing the filter

95 photometer measurements with those obtained by thermal-optical analysis (Sciare, 2011). However,

96 as the determination of elemental carbon (EC) depends on the thermal-optical analysis method,

97 sometimes with large differences (Bae et al., 2009), the determination of the mass absorption cross-

98 section also depends on the thermal-optical method employed. Additionally, the season and the

99 sample composition (Bae et al., 2009; Chiappini et al., 2014) may influence the determination of EC;

100 and the mass absorption cross-section may depend on the aerosol mixing state and size (Bond and

101 Bergstrom, 2006). Concurrent determination of EC in filter samples with an thermal-optical method,

102 and the Aethalometer measurement of optical absorption allow the site-specific determination of

103 the mass absorption cross-section, which is specific to the thermal-optical method employed – this

104 procedure is often employed in source apportionment campaigns, where mass closure is attempted

105 (Sciare, 2011).

106

107 **References**

108 Bae, M.-S., Schauer, J. J., Turner, J. R., Hopke, P. K., Seasonal variations of elemental carbon in urban

109   aerosols as measured by two common thermal-optical carbon methods, Sci. Tot. Environ.

110   407, 5176–5183, doi:10.1016/j.scitotenv.2009.05.035, 2009.

111 Bond, T. C. and Bergstrom, R. W.: Light absorption by carbonaceous particles: An investigative

112   review, Aerosol Sci. Technol., 40, 27–67, 2006.

113 Chiappini, L., Verlhac, S., Aujay, R., Maenhaut, W., Putaud, J. P., Sciare, J., Jaffrezo, J. L., Liousse, C.,

114   Galy-Lacaux, C., Alleman, L. Y., Panteliadis, P., Leoz, E., and Favez, O.: Clues for a standardised

115   thermal-optical protocol for the assessment of organic and elemental carbon within ambient

116   air particulate matter, Atmos. Meas. Tech., 7, 1649-1661, doi:10.5194/amt-7-1649-2014,

117   2014.

118 Fialho, P., Hansen, A. D. A., Honrath, R. E., Absorption coefficients by aerosols in remote areas: a new

119   approach to decouple dust and black carbon absorption coefficients using seven-wavelength

120   Aethalometer data, J. Aerosol Sci., 36, 267-282, 2005.

121 Gundel, L. A., Dod, R. L., Rosen, H., and Novakov, T.: The relationship between optical attenuation

122   and black carbon concentration for ambient and source particles, Sci. Total Environ., 36, 197–

123   202, doi:10.1016/0048-9697(84)90266-3, 1984.

124   Moosmüller, H., Chakrabarty, R. K., Ehlers, K. M., and Arnott, W. P.: Absorption Ångström coefficient,

125   brown carbon, and aerosols: basic concepts, bulk matter, and spherical particles, Atmos.

126   Chem. Phys., 11, 1217-1225, doi:10.5194/acp-11-1217-2011, 2011.

127   Sandradewi, J., Prévôt, A. S. H., Weingartner, E., Schmidhauser, R., Gysel, M., Baltensperger, U.: A

128   study of wood burning and traffic aerosols in an Alpine valley using a multi-wavelength

129   aethalometer, Atmos. Environ., 42, 101-112, 2008a.

130   Sandradewi, J., Prévôt, A. S. H., Szidat, S., Perron, N., Alfarra, M. R., Lanz, V. A., Weingartner, E., and

131   Baltensperger, U.: Using aerosol light absorption measurements for the quantitative

132   determination of wood burning and traffic emission contributions to particulate matter,

133   Environ. Sci. Technol., 42, 3316–3323, doi:10.1021/es702253ms, 2008b.

134   Sciare, J., d' Argouges, O., Sarda-Estève, R., Gaimoz, C., Dolgorouky, C., Bonnaire, N., Favez, O.,

135   Bonsang, B., and Gros, V.: Large contribution of water-insoluble secondary organic aerosols

136   in the region of Paris (France) during wintertime, J. Geophys. Res.-Atmos., 116, D22203,

137   doi:10.1029/2011JD015756, 2011.

138   Yang, M., Howell, S. G., Zhuang, J., and Huebert, B. J.: Attribution of aerosol light absorption to black

139   carbon, brown carbon, and dust in China – interpretations of atmospheric measurements

140   during EAST-AIRE, Atmos. Chem. Phys., 9, 2035-2050, doi:10.5194/acp-9-2035-2009, 2009.